

# Mass Transfer in Packed Beds Operated Cocurrently

C.Y. WEN and WILLIAM S. O'BRIEN  
West Virginia University, Morgantown, W. Va.

LIANG-TSENG FAN  
Kansas State University, Manhattan, Kan.

**Conventional operation of packed towers has been the countercurrent passage of the phases through the bed, the liquid falling downward through and over the packing, with the gas phase moving upward through the bed. This study provides mass transfer (dehumidification) data in cocurrent flow packed towers using the various sizes of Raschig rings.**

CONVENTIONAL OPERATION of packed towers has been the countercurrent passage of the phases through the bed, the liquid falling downward through and over the packings, with the gas phase moving upward through the bed (4). The countercurrent operation of the bed produces a greater driving force than the cocurrent operation between the phases and thus produces a greater mass transfer rate, since the rate is directly proportional to the driving force. This advantage is illustrated in Figure 1, indicating the relationship of the concentration of the transferred material within each phase corresponding to the packing height. The concentration relationship for the countercurrent operation is compared with the relationship for the cocurrent operation in which both phases are moving together downward through the packed bed. The mean driving force for the countercurrent operation, is higher than that of the cocurrent operation.

However, if the concentration or partial pressure of the active material in one phase remains constant due to a chemical reaction rendering the active material inert upon absorption (as in the case of the absorption of  $\text{CO}_2$  by a water-NaOH solution) or if, because of a very large difference in mass flow rates of the two phases, the change in concentration of one phase is negligible as in the case of the dehumidification of air by  $\text{CaCl}_2$  solution, the concentration to bed height relationship in both the countercurrent and cocurrent flow patterns are quite similar. This relationship, illustrated by Figure 2, presents an argument that with systems having those conditions of a constant active concentration in one of the phases, the cocurrent operation of the packed bed might be comparable to the countercurrent operation.

In the countercurrent operation of a packed bed, the flow rate ranges of the phases are limited by the flooding point of the column, at which either the liquid rate is too great to allow the gas flow to proceed up the column, or the gas rate is too great to permit the downward flow of the liquid. This flooding point places an operational limit upon the capacity of the column. In contrast, in the cocurrent operation, the column has no such maximum limit of the column capacity with cocurrent flow, quite large flow of both phases can pass through the packed bed far in excess of the countercurrent flooding point.

The cocurrent packed bed operation has usage also as a reactor for heterogeneous liquid-gas reactions. The passage of the phases downward over the packings serves to promote an intimate contact of the phases without outside agitation, while giving the advantage of a flow reactor to decrease the backmixing which, in some cases, decreases the yield. In addition, the packing particles could be constructed of a material which has a favorable catalytic effect on the reaction, giving simultaneous intimate contacting of the reactants and the catalyst.

Realizing the possible advantages of the cocurrent packed bed system, this study was undertaken to provide mass transfer data in cocurrent flow packed towers.

A study of cocurrent mass transfer in packed beds was undertaken by Dodds (2). Choosing the absorption of

carbon dioxide by a water solution of sodium hydroxide as the system, Dodds investigated five contributing factors to the mass transfer rates. The five factors were packing type, temperature, sodium solution normality, gas rate, and liquid rate. The absorption tower was 18 inches in diameter with a five-foot packed section. The five types of tower packings used were 1-inch and 1.5-inch Berl saddles, 1-inch and 1.5-inch Intalox saddles, and 2-inch steel rings. Two liquid rates, two gas rates, two levels of sodium solution normality, and two temperatures were investigated statistically. The analysis of the results indicated a significant variance of the mass transfer coefficient with each of the five factors investigated as well as several significant interactions among gas rate, liquid rate, and temperature. The author did not obtain a mathematical design correlation for the effect of the five factors, but established the significance of each of the factors, coefficient.

In a 1960 article based on the same experimental data, Dodds illustrated the effect of the five factors mentioned earlier on the trends of the mass transfer coefficients (3).

In 1956 McIlvriod (5) studied the desorption of oxygen from water into air during the downward cocurrent flow of the air and the water phases through a packed bed. The studies covered three types of packings:  $\frac{1}{4}$ -inch ceramic Raschig rings, and 4- and 6-mm. glass beads. The gas rates studied ranged from 400 to 4000 lb./sq. ft. hr.

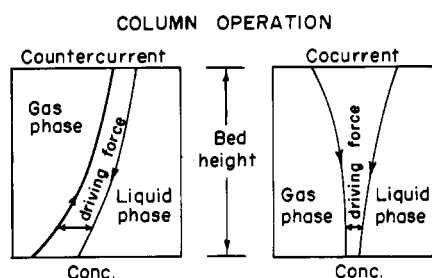


Figure 1. Phase concentration vs. bed height with both phase concentrations changing

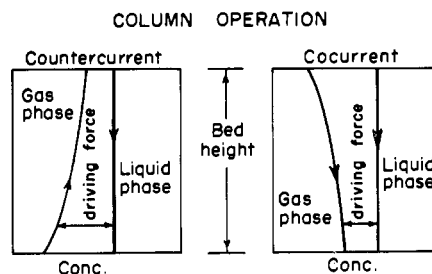


Figure 2. Phase concentration vs. bed height with one phase concentration constant

and the liquid rate varied from 7080 to 94,350 lb./sq. ft. hr. The packed bed was contained in 2-inch I.D. lucite tubing constructed in flanged section allowing the height of the packed bed to be varied. The variation of bed height was shown to have no effect on the resultant mass transfer coefficient; however, the range of bed height was varied only from 1.88 to 4.50 inches, a rather small over-all height of packing.

Plotting on logarithmic coordinates the resultant liquid mass transfer coefficient,  $k_L a$  (the unit in  $\text{hr.}^{-1}$ ) vs. the gas mass rate, two distinct transfer mechanisms were indicated with the glass beads as the packing material, but only one mechanism was present for the  $\frac{1}{4}$ -inch rings. The mechanism, indicated by straight lines on the log-log plots, was generally explained by the author. The mechanism at the lower gas rates was explained as due to a rapid thinning of the liquid film with a corresponding decrease in the time of contact and increase in  $k_L a$ . Also, as the gas rate was increased, there was a more even distribution of the liquid phase with an increase in the effective wetted area available for mass transfer. A point was reached at which essentially all of the available area was completely wetted. With higher gas rates, the effect of the gas rate on  $k_L a$  was less pronounced since it was only due to the continual decrease in film thickness, and/or the increased turbulence caused by the increasing rates. The presence of only one mechanism with the rings was explained as due to the hollow shape which prevented a completely even distribution of the phases throughout the packing. The author correlated the results empirically as function of gas and liquid flow rates.

Collins (1) studied the absorption of carbon dioxide in a cocurrent wetted wall column and compared the results with a countercurrent operation. The film thickness of the liquid film flowing down the column was measured by photographic means and correlated in terms of the flow rates.

#### METHOD OF CALCULATION

In the interphase mass transfer, the rate of mass transfer is expressed as directly proportional to the driving force and interphase area and inversely proportional to the resistance encountered in the passage mechanism.

The mass transfer operation involving the air-water system is a specialized type known as humidification or dehumidification, depending on whether water is added or removed from the air stream. The most convenient driving force units for this particular system are in terms of the humidity of the air stream. The air humidity can be calculated as

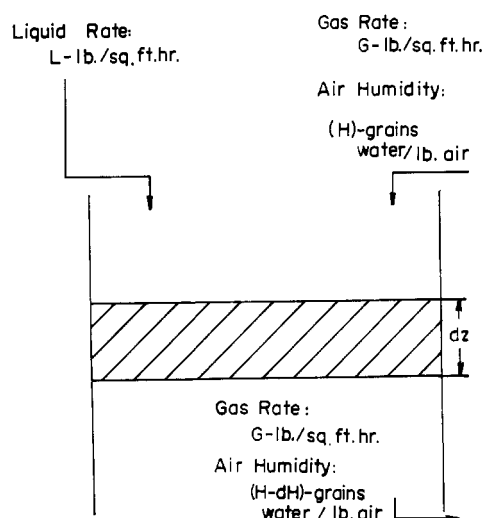
$$H = \frac{P_w}{P - P_w} \frac{M_w}{M_a} \quad 7000 \quad (1)$$

where

- $H$  = air humidity, grains water/lb. dry air
- $P_w$  = partial pressure of water in air
- $P$  = total pressure of the system
- $M_w$  = molecular weight of water, 18
- $M_a$  = molecular weight of air, 28.97

The driving force which actuates the mass transfer is defined as the difference between the air humidity and the equilibrium humidity based on the properties of the liquid present. The equilibrium humidity is calculated by the previous humidity formula, using the vapor pressure of the solution in place of the partial pressure of the water in the air.

The derivation of the operational formula for correlation proceeds on a semitheoretical bases. Choosing an axial portion of the system flow path as the model, the operation of the dehumidification can be illustrated as



For isothermal conditions, the rate of moisture removed from the air through a differential packed bed height,  $dz$ , is

$$-G(dH) = K_{Ha}(H - H^*)dz \quad (2)$$

In the dehumidification of air with calcium chloride solution, the resistance encountered by the passage of water from the interface into the solution is negligible compared to the resistance of the water passage from the air bulk stream to the air-liquid interface. Thus, the interfacial liquid stream concentration, and the system can be termed as gas film controlling.

The surface area factor is normally considered with the mass transfer coefficient as a combined volumetric coefficient as a combined volumetric coefficient,  $K_{Ha}$  (4). From Equation 2

$$-G \frac{dH}{H - H^*} = (K_{Ha})dz \quad (3)$$

assuming the equilibrium humidity,  $H^*$ , as a constant property (the concentration and temperature change are quite negligible with passage through the column) the above equation can be integrated for a packed bed height of  $z$  and an air stream entrance humidity of  $H_i$  and exit humidity of  $H_o$  with the resulting formula

$$z = \frac{G}{K_{Ha}} \ln \frac{H_i - H^*}{H_o - H^*} \quad (4)$$

The formula for the column height has been divided into two factors: the number of transfer units and the height of a transfer unit. The number of the transfer units is termed  $N$ , and refers to that portion of the design equation,  $N = \ln (H_i - H^*) / (H_o - H^*)$ . The height of a transfer unit,  $H_{OG}$ , is the height of packed column necessary to transfer the equivalent of one mass transfer unit. In the design formula  $H_{OG} = G / K_{Ha}$ . Since the number of transfer units is a function only of the driving force, the effect of the external factors involved in the column operation is indicated only in the transfer unit height; therefore, that height must be correlated as a function of gas rate, liquid rate, and column packing structures and arrangements.

The additional mass transfer taking place outside the bed is known as end effect and can be measured by the number of transfer units of mass moved, because that unit is not affected by the shape or type of the operational contactor. By the subtraction of the end effect number of transfer units,  $N_e$ , from the total number of units transferred,  $N'$ , the number of units transferred within the packing alone,  $N$  can be calculated. This end effect number of units was measured by placing the phase distributor flush against the bottom of the column without packings and thus separating the

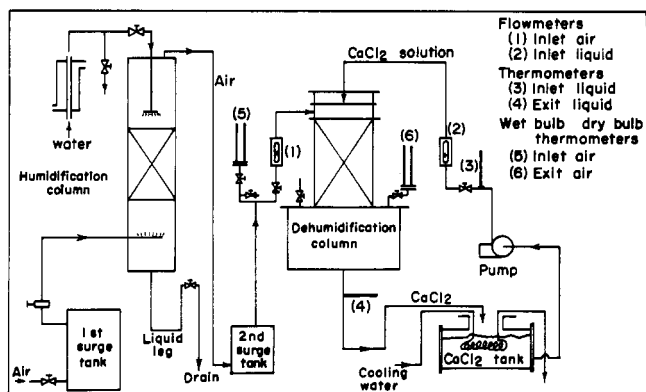


Figure 3. Dehumidification equipment flowsheet

phase immediately after the emergence from the distributor.

A description of the expected effects of the external factors upon the mass transfer is compared with the experimental trends in the later section.

## EQUIPMENT

Apparatus (Figure 3) for the mass transfer operation consists of the auxiliary equipment necessary in the preparation, metering, and analysis of both the incoming air stream and calcium chloride solution, and of the main dehumidification column.

**Air Preparation Equipment.** From the supply line, the air entered the first surge tank, 19 inches in diameter and 3 feet in height. In this tank, condensible oil and liquid water particles in the air were removed, and the large volume of the tank helped to maintain a constant pressure on the air supply. The tank was equipped with a 3/4-inch steam trap to remove the accumulated entrainment.

Air flow from the surge tank to the humidification column was controlled by a pressure-regulating valve. The purpose of this column was dual: to raise and control the humidity of the air to its maximum value and to control the temperature of the air to a value in the region of the temperature of the liquid solution and surrounding atmosphere. This control was accomplished by mixing heated water with the air stream in a countercurrent packed bed. The water, from the city water supply, was heated by a steam-heated, single-tube copper heat exchange, a 2-inch diameter shell covering a 3/4-inch diameter tube, 32 inches long. The water temperature was controlled by varying the water flow through the exchanger. The column was made of two 2-foot long, 5-inch diameter pyrex glass pipes, packed 18 inches high, with 1-inch porcelain Intalox saddles. The column was provided with a 55-inch leg with a 2-foot indirect sight glass. A valve located on the leg maintained a water level, forcing the gas upward through the packing.

The humid air then entered a second surge tank. This tank removed any water entrainment carried over the humidification column. The location of the tank prevented the entrained water stream from proceeding through the gas measuring flowmeter and thermometers.

By regulating in the humidification column, a fairly constant inlet air humidity was maintained throughout the entire operating time.

The humidity-measuring apparatus for the air stream consisted of two thermometers mounted into the end of a 1.5-inch pipe fixture with the thermometer stems exposed for reading. One stem was covered with a cloth wick leading through a hole in the pipe wall to a small bottle of distilled water mounted to the outside of the pipe. The thermometers measured from  $-10^{\circ}$  to  $50^{\circ}$  C. and had 0.1 degree subdivisions. The air flow through the pipe operated the wick-covered thermometer as a wet bulb temperature

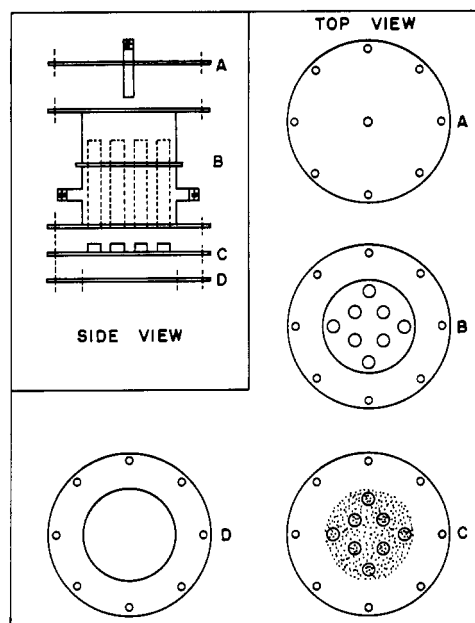


Figure 4. Two-phase cocurrent distributor

device, allowing the humidity of the air to be calculated by the standard humidity charts. A duplicate of the pipe-and-thermometer apparatus was used on the exit air stream from the dehumidification column to measure the humidity of the outlet air. The air flow to the dehumidification column was metered by a flowmeter.

**Calcium Chloride Solution Equipment.** The bulk calcium chloride solution supply was contained in a horizontal lead-lined tank. The solution tended to gradually increase in temperature over an operating time due to a high heat of mixing. A cooling coil of spiraled 3/8-inch copper tubing was placed in the solution tank to reduce the heating effect. The calcium chloride solution temperature was maintained most of the time within  $25^{\circ}$  to  $28^{\circ}$  C.

The solution was forced through the process system by a pump. The solution temperature was measured both before entering and after leaving the dehumidification column. The liquid temperature usually remained constant with passage through the packed bed, but increases of 1 to 2 degrees were noted with the lower flow rates.

The concentration of the solution was determined from the density by a precision hydrometer, with 0.0005 subdivisions and a range of 1.350 to 1.4300 sp. gr.

**Dehumidification Column.** The main dehumidification column consisted of a glass shell 6 inches in diameter upon which the two-phase distributor was seated. The distributor (Figure 4), was divided into two compartments. The liquid

Table I. Tower Packing Specifications (4)

Type	Size, Inches	Wall Thickness, Inches	Approx. Quantity/Cu. Ft.	Approx. Surface Area, Sq. Ft./Cu. Ft.	Free Gas Space, %
Raschig Rings					
Carbon	1/4	1/16	85,000	212	55
Porcelain	1/2	1/16	10,600	114	74
Porcelain	1	1/8	1,350	58	73
Intalox Saddles					
Porcelain	1/2	1/4	20,700	190	78
Porcelain	1	1/8	2,385	78	77.5
Berl Saddles					
Porcelain	1	1/8	16,200	142	63
Porcelain	1	1/4	2,200	76	69

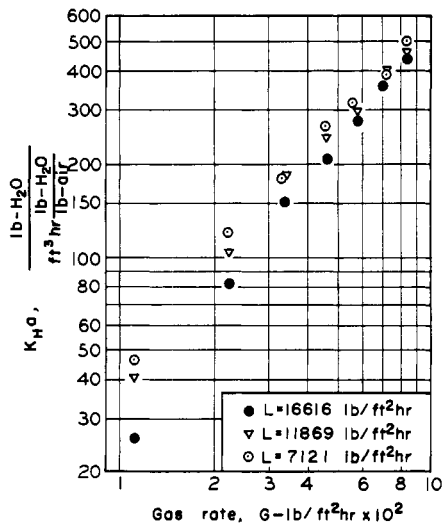


Figure 5.  $K_{Ha}$  vs. gas rate; 1-inch Rasching rings

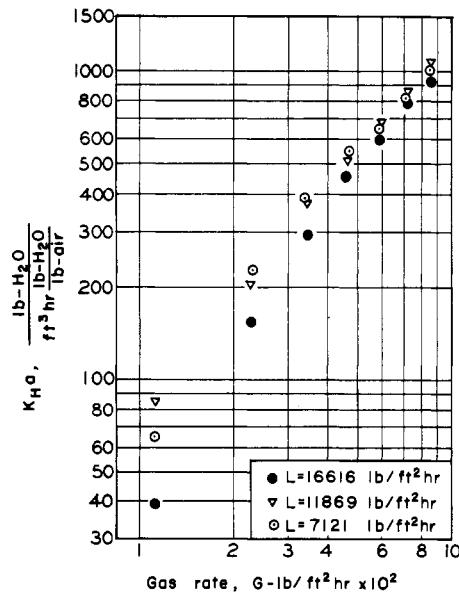


Figure 6.  $K_{Ha}$  vs. gas rate;  $\frac{1}{2}$ -inch Rasching rings

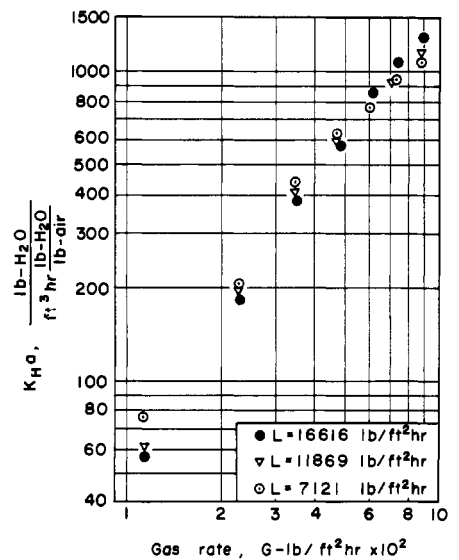


Figure 7.  $K_{Ha}$  vs. gas rate;  $\frac{1}{4}$ -inch Rasching rings

entered the top chamber and through the inside of the eight tubes where it was sprayed by the perforated distributor plate into the packing. The air phase entered the second chamber through two entrance pipes for better distribution. The air passed through the distributor plate into the packing through the area surrounding the liquid tubes. The distributor plate was made of  $\frac{1}{8}$ -inch steel plate; the center section, 6-inches in diameter, was entirely perforated with  $\frac{1}{8}$ -inch holes. The two phases were distributed as they passed through the plate except for very low liquid rates. For this reason, the lowest liquid rate was eliminated from the experimental procedure.

The packing was enclosed by a double-touch borosilicate glass pipe, 6 inches in diameter. The shell was made in flanged 1-foot sections allowing the effect of packing height on the mass transfer rate to be determined.

The phases, after passing through the packing, were separated upon the entrance into a drum, 16 inches in diameter, located directly below the packed section. Due to a sudden reduction of linear velocity, the two phases were totally separated; the air phase passed through 1-inch pipes on the top of the drum, and the liquid passed through the drum bottom, through a liquid leg to eliminate air flow, and returned to the bulk solution tank.

The tower packings used were manufactured by the U. S. Stoneware Co. with specifications listed in Table I.

### EXPERIMENTAL PROCEDURE

The equipment was started with the operation of the countercurrent dehumidification column. The desired temperature and flow rate of the humidifying water were established to produce the humid air temperature within one or two degrees of the room temperature and the liquid bulk temperature. The column was operated a few minutes to stabilize the resultant air conditions before the valve to the dehumidification column was opened.

For a particular packing type and bed height, 39 runs were made, with 30 combinations of gas and liquid rates and 9 repeat runs for reproducibility. During the taking of the data, the particular combination of rates to be run was picked randomly from the set of runs.

The desired flow rates were set and maintained constantly for a time period of 7 to 10 minutes to ensure the stability of the flow pattern. During the run time, the instruments were periodically checked for radical changes in the variables indicating a procedure error. If such a change was noted, the error was corrected and run remade. The samples were taken from the solution line at the point where the solution from the dehumidification column enters the bulk solution tank.

The concentration of the calcium chloride solution changed only very slightly, making the reconcentration of

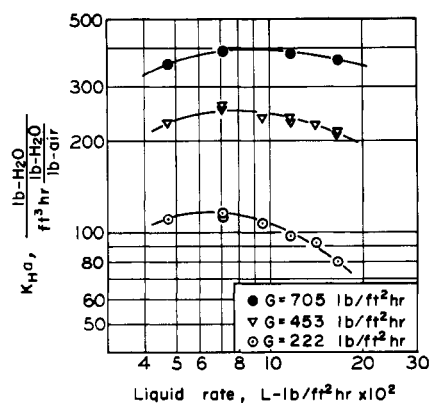


Figure 8.  $K_{Ha}$  vs. liquid rate; 1-inch Rasching rings

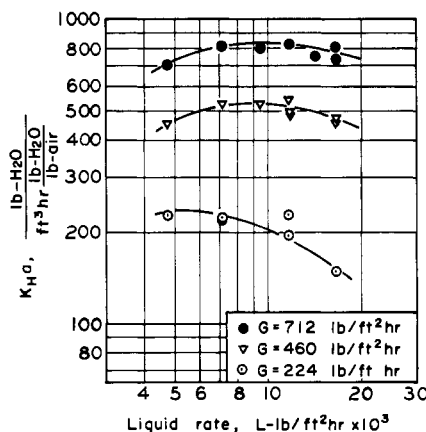


Figure 9.  $K_{Ha}$  vs. liquid rate;  $\frac{1}{2}$ -inch Rasching rings

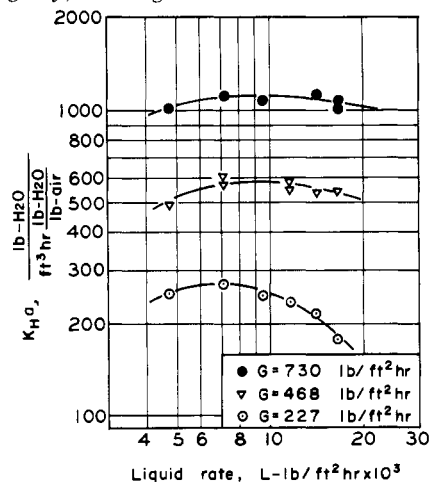


Figure 10.  $K_{Ha}$  vs. liquid rate;  $\frac{1}{4}$ -inch Rasching rings

the solution necessary only after several series of runs. The solution concentration was maintained in the general region of 39 to 41% by weight  $\text{CaCl}_2$ .

## DISCUSSION

The values of  $K_{HA}$  were plotted against gas rate in Figures 5, 6, and 7 for the packed beds of 1-,  $\frac{1}{2}$ -, and  $\frac{1}{4}$ -inch Raschig rings, respectively. The 1-inch ring bed was 2 feet high; the  $\frac{1}{2}$ -inch and  $\frac{1}{4}$ -inch Raschig rings, respectively. The 1-inch ring bed was 2 feet high; the  $\frac{1}{2}$ -inch and  $\frac{1}{4}$ -inch ring beds were 1 foot high. The effects of liquid rates on  $K_{HA}$  were plotted in Figures 8, 9, and 10.

In the dehumidification operation the number of transfer units varied only slightly with different gas and liquid rates. Since the logarithmic term varies only slightly, the gas mass rate has a direct influence on the coefficient (Figures 5, 6 and 7).

At constant gas rates, the values of  $K_{HA}$  decreased with increasing liquid rates, as shown in Figures 8, 9, and 10, except for the lowest liquid rate. This was probably due to the fact that at higher liquid rate, the liquid stream would tend to form a channeled path easier than at a lower rate. Therefore, at a high liquid rate in which the space void of liquid was small, the interphase turbulence may be reduced, and the gas phase would be compressed into a smaller volume with a corresponding smaller contact surface area, resulting in a reduction of the mass transfer rate. The channeling phenomenon is quite possible in the dispersed phase regions described in the previous section. The effect of an increase in the  $K_{HA}$  value with an increase in liquid rate at the lower liquid rate region could be due to the incomplete turbulence of the phase before the dispersed phase was formed. In this region, the liquid rate would have a greater mixing effect on the mass transfer rates.

The effect of the liquid rates was more pronounced at the lowest gas rate ( $G = 225 \text{ lb./sq. ft. hr.}$ ) than at the higher

gas rates. This was probably due to the additional decrease in contact area because of the tendency of channeling at the low gas rate.

The trends of the height of a transfer unit vs. varying liquid rates (Figures 11, 12, and 13) indicate a similar mechanism as the effect of liquid rate on  $K_{HA}$ . As the height of a transfer unit decreases (increasing mass transfer rate) at the lower liquid rates, a minimum transfer height with increasing liquid rates was noted.

The transfer unit height decreased with increasing gas rates (Figures 14, 15, and 16). This increase in the mass transfer rate was due to the increasing interphase turbulence with increasing gas rates. The greater gas rates tend to break up the liquid stream, exposing a greater interfacial surface area available for mass transfer. A minimum height was reached, particularly noted in the  $H_{OG}$  vs.  $G$  curves for  $\frac{1}{4}$ -inch Raschig rings (Figure 16). At this region the increasing turbulence caused by the increasing flow rates reached a limit, and the effect of the decreasing contact area of the phases began to control the mechanism. This minimum transfer height, and consequently the maximum mass transfer rate of the column operation, seemed to be independent of the liquid rate.

The assumption that the average driving force can be represented as a logarithmic mean is applicable only when there is no axial diffusion taking place. This assumption would be quite reasonable if the change in concentration of the transferred material in one phase was small in comparison with the driving force. However, in this operation the dehumidification of the air stream to equilibrium humidity was very nearly complete. The exact form of the operating curve would therefore have a great bearing on the adaptability of the formula for design purposes.

The derivation of the mass transfer formula also assumes that the mass transfer coefficient,  $K_{HA}$ , was constant throughout the operating column with a given set of conditions. If the flow were completely uniform throughout the

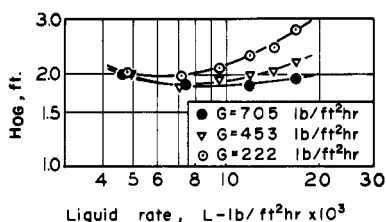


Figure 11.  $H_{OG}$  vs. liquid rate; 1-inch Raschig rings

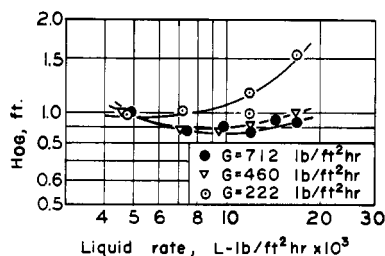


Figure 12.  $H_{OG}$  vs. liquid rate;  $\frac{1}{2}$ -inch Raschig rings

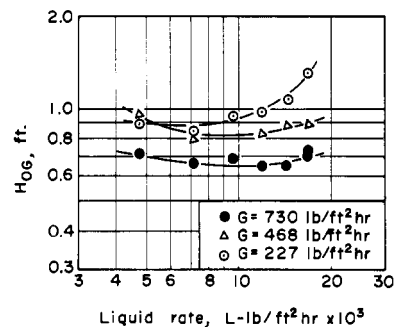


Figure 13.  $H_{OG}$  vs. liquid rate;  $\frac{1}{4}$ -inch Raschig rings

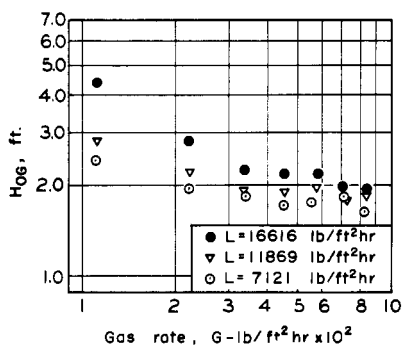


Figure 14.  $H_{OG}$  vs. gas rate; 1-inch Raschig rings

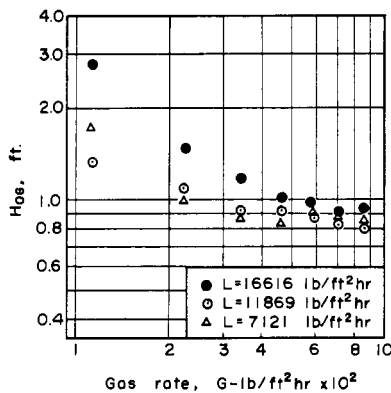


Figure 15.  $H_{OG}$  vs. gas rate;  $\frac{1}{2}$ -inch Raschig rings

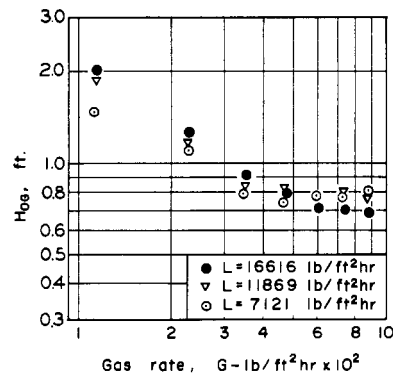


Figure 16.  $H_{OG}$  vs. gas rate;  $\frac{1}{4}$ -inch Raschig rings

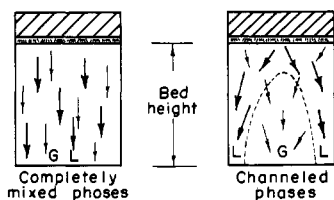


Figure 17. Flow patterns within cocurrent packed beds

bed, this assumption would be correct. However, a visual observation of the flow patterns indicates an accumulation of the liquid phase near the wall after passage through about 1 foot of the packing. An explanation of this pattern would be a tendency of the higher gas rates to force the liquid into the annulus channel near to the wall surrounding the gas channels moving down the center of the column. This channeling would reduce the interphase turbulence as the phases move down the bed, decreasing the interfacial surface area,  $a$ , and thus would decrease the mass transfer coefficient  $K_f a$ . This separation of the phases was illustrated in Figure 17.

The reduction in the mass transfer rate with respect to column height was indicated in Figure 18, showing the number of mass transfer units exchanged in each foot of a 2-foot bed of  $\frac{1}{4}$ -inch Raschig rings with constant gas and liquid mass rates.

The comparatively greater interphase turbulence at the entrance portion of the bed producing a greater mass transfer would produce a skewed form of the operating-equilibrium curves than the curves assumed by the logarithmic mean driving force.

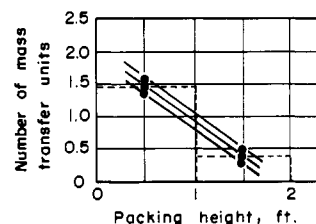


Figure 18. Mass transfer units vs. packing height

#### LITERATURE CITED

- (1) Collins, D.E., Ph.D. dissertation, Prudue University, Lafayette, Ind. 1958.
- (2) Dodds, W.S., Ph.D. dissertation, Northwestern Univ., Evanston, Ill. 1953.
- (3) Dodds, W.S. Stutzman, L.F., Sollami, B.J., R.J. McCarter, *A.I.Ch.E. J.* 6, 197, 1960.
- (4) Leva, Max, United States Stoneware Co., Akron, Ohio, Bull. TP 54, 1951.
- (5) McIlvriod, H.G., Ph.D. dissertation, Carnegie Inst. Technol., Pittsburgh, Pa., 1956.

RECEIVED for review April 23, 1962. Accepted August 24, 1962.

Material supplementary to this article has been deposited as Document No. 7378 with the ADI Auxilliary Publications Project, Photoduplication Service, Library of Congress, Washington 25, D. C. A copy may be secured by citing the document number and by remitting \$1.25 for photoprints or \$1.25 for 35-mm. microfilm. Advance payment is required. Make checks or money orders payable to Chief, Photoduplication Service, Library of Congress.

## Pressure Drop Through Packed Beds Operated Cocurrently

C. Y. WEN, WILLIAM S. O'BRIEN,  
West Virginia University, Morgantown, W. Va.

LIANG-TSENG FAN,  
Kansas State University, Manhattan, Kan.

This article provides pressure drop data through packed towers under cocurrent operation and by use of the following packings:  $\frac{1}{4}$ -inch Raschig rings,  $\frac{1}{2}$ -inch Raschig rings,  $\frac{1}{2}$ -inch Berl saddles,  $\frac{1}{2}$ -inch Intalox saddles, 1-inch Raschig rings, and 1-inch Intalox saddles. A correlation for the continuous gas phase-dispersed liquid phase region is empirically presented. Constants are obtained for each packing, as well as for different fluid properties; therefore, this form cannot be directly extended into other packing or fluid systems without further investigations. However, the data fit the empirical formula well.

THE COMMON OPERATION of packed columns has been the countercurrent operation (4); however, cocurrent operation can be advantageously employed in some cases (7). This article provides pressure drop data through packed towers under cocurrent operation.

The first collection of pressure drop data over a packed bed with a cocurrent system was done by Dodds (1). Using 1-inch and 1.5-inch Berl saddles and Intalox saddles, and 2-inch steel rings as packing material in an 18-inch diameter column, the author measured the cocurrent pressure drop and holdup of two systems air-water and air-2.5N  $\text{Na}_2\text{CO}_3$  (liquid density, 1.12). The mass rates measured were: liquid range, 4250 to 33,350 lb./sq. ft. hr. and air range, 197 to 1810 lb./sq. ft. hr. Dodds did not correlate the data, but only presented it in tabular and graphical form as a reference. In 1960 article, he and co-authors presented the

data for both pressure drop and liquid holdup in a graphical form (2).

The first correlation for the cocurrent pressure drop in packed beds was presented by McIlvriod (6). With a 2-inch diameter column packed with 4-mm. and 6-mm. glass beads and  $\frac{1}{4}$ -inch Raschig rings, liquid flow rates from 7080 to 94,350 lb./sq. ft. hr. and gas mass rates from 400 to 4000 lb./sq. ft. hr. were investigated. The height of packing was varied with a maximum height of 4.50 inches. The pressure drop data were plotted on log-log coordinate paper resulting in two distinct zones. The lower zone was an unsteady pulsating flow occurring at low gas to liquid ratios. At higher gas to liquid ratios, another zone existed which was divided into three regions. A break point existed in the pressure drop vs. gas rate curve using constant liquid rates as the parameter. The three regions defined were liquid